

## Doping profile and Ge-dose optimization for silicon–germanium heterojunction bipolar transistors

This content has been downloaded from IOPscience. Please scroll down to see the full text.

2009 Semicond. Sci. Technol. 24 105020

(<http://iopscience.iop.org/0268-1242/24/10/105020>)

View [the table of contents for this issue](#), or go to the [journal homepage](#) for more

Download details:

IP Address: 140.113.38.11

This content was downloaded on 25/04/2014 at 07:27

Please note that [terms and conditions apply](#).

# Doping profile and Ge-dose optimization for silicon–germanium heterojunction bipolar transistors

Yiming Li<sup>1,2,3,4</sup>, Ying-Chieh Chen<sup>1</sup> and Chih-Hong Hwang<sup>1</sup>

<sup>1</sup> Institute of Communication Engineering, National Chiao-Tung University, Hsinchu 300, Taiwan

<sup>2</sup> Department of Electrical Engineering, National Chiao-Tung University, Hsinchu 300, Taiwan

<sup>3</sup> National Nano Device Laboratories, Hsinchu 300, Taiwan

E-mail: [yml@faculty.nctu.edu.tw](mailto:yml@faculty.nctu.edu.tw)

Received 26 May 2009, in final form 17 July 2009

Published 22 September 2009

Online at [stacks.iop.org/SST/24/105020](http://stacks.iop.org/SST/24/105020)

## Abstract

The speed of silicon–germanium (SiGe) heterojunction bipolar transistors (HBTs) has been dramatically increased. It is known that the speed of HBTs is dominated by the base transit time, which could be influenced by the doping profile in the base region and the Ge concentration. In this study, the design of the doping profile and Ge-dose concentration for SiGe HBTs are mathematically formulated and solved by a technique of geometric programming (GP). The solution calculated by the GP method is guaranteed to be a global optimal. The accuracy of the adopted numerical optimization technique is first confirmed by comparing with two-dimensional device simulation. The result of this study shows that a 23% Ge fraction may maximize the current gain; furthermore, a 12.5% Ge may maximize the cut-off frequency for the explored device, where a 254 GHz cut-off frequency is achieved.

(Some figures in this article are in colour only in the electronic version)

## 1. Introduction

The basis of silicon–germanium (SiGe) technology is SiGe heterojunction bipolar transistors (HBTs), which exhibits various merits over conventional Si bipolar and silicon metal-oxide-semiconductor field effect transistors for implementation of high-frequency circuits. SiGe HBTs have undergone substantial development for nearly two decades. The operation speed of SiGe HBTs has increased dramatically, with the consequence of relentless vertical and lateral scaling. The HBTs' operation speed is mainly dominated by the transit time of base, which is strongly influenced by the doping profile and Ge concentration in the base region [1–18]. The determination of the doping profile and Ge concentration of the base region is thus crucial for optimal design of SiGe HBTs in advanced communication circuits. Diverse engineering and theoretical approaches have been proposed to optimize the base transient time through optimization of the base doping profile [3–12]. An analytical optimum base doping profile

by using variational calculus considering the dependence of diffusion coefficient on base doping concentration was derived [3]. The analytical approach has been extended to consider the dependence of intrinsic carrier concentration on base doping concentration [4]. An iterative approach has also been proposed to obtain the optimum base doping profile [5], where the dependence of mobility and bandgap narrowing on the base doping concentration was considered [6]. Unfortunately, the solution cannot be guaranteed to be the global optimal result. Consequently, if the problem can be modeled as an optimization problem and solved for a global solution, it may benefit the SiGe technology.

A geometric programming (GP) is a type of mathematical optimization problem that is characterized by objective and constraint functions with a certain special mathematical form. Recently, numbers of practical problems, particularly in semiconductor and electrical circuit design, have been found to be equivalent (or can be well transformed) to GP's form [19–31]. A new approach, interior-point algorithms, has also been proposed to solve the large-scale GP problem efficiently and reliably [19], which significantly benefits the development

<sup>4</sup> Author to whom any correspondence should be addressed.

of advanced semiconductor and electrical circuit design. For the SiGe HBTs, it has been reported that the triangular Ge profiles are best suited to achieve the minimum base transit time and trapezoidal Ge profiles are best suited to get high current gain in SiGe HBTs [18]. The GP approach has recently been utilized to simultaneously optimize the Ge-dose and base doping profile in SiGe HBTs [1, 2]. However, the co-optimization of cut-off frequency and current gain in SiGe HBTs are still lacked.

In this work, the GP approach is advanced to pursue the optimal Ge-dose as well as the doping profile for the high cut-off frequency or the high current gain in SiGe HBTs. The design of HBTs is first expressed as a special form of an optimization problem, the so-called GP, which can be transformed to a convex optimization problem, and then solved efficiently. The background doping profile is adjustable to improve the cut-off frequency and current gain. The result shows that a 23% Ge fraction may maximize the current gain, where a factor, current gain divided by the emitter Gummel number, of 1100 is attained. Furthermore, to maximize the cut-off frequency of HBTs, a Ge-dose concentration of 12.5% is used, where the cut-off frequency can achieve 254 GHz. Note that the accuracy of the developed optimization technique has been confirmed by comparing it with that of a two-dimensional (2D) device simulation. This study successfully considers the device characteristics and manufacturing limitation as a GP model and the result may provide an insight into the design of SiGe HBTs.

This paper is organized as follows. In section 2, the GP formulation of the design of HBTs and manufacturing limitation are described. In section 3, the optimized cut-off frequency and current gain are discussed according to the calculated results. Finally, we draw conclusions and suggest future work.

## 2. Solution methodology

Figure 1 shows the studied SiGe HBTs device for the doping profile and Ge-dose concentration co-design, and also for a 2D device simulation. Mathematically, a doping profile tuning problem for the high-frequency property optimization of SiGe HBTs can be formulated as an optimization problem:

$$\begin{aligned} & \text{Maximum } f_t \\ \text{s.t. } & N_{\min} \leq N_A(x) \leq N_{\max}, \quad 0 \leq x \leq W_B \\ & 0 \leq G(x) \leq G_{\max}, \quad 0 \leq x \leq W_B \\ & \text{Ge}_{\text{AVG}} = \frac{1}{W_B} \int_0^{W_B} G(x) dx \end{aligned} \quad (1)$$

where  $f_t$  is the cut-off frequency;  $N_A(x)$  and  $G(x)$  are the base doping profiles for silicon and germanium respectively, which are spatial-dependent positive functions over the interval  $0 \leq x \leq W_B$  and  $x$  is the depth from the interface of base and emitter into the substrate. The base doping profile of silicon is lower than the doping level of emitter-base junction,  $N_{\max}$ , and higher than the background doping,  $N_{\min}$ . The base doping profile of germanium is less than the maximum value  $G_{\max}$ , and  $\text{Ge}_{\text{AVG}}$  is the average value of Ge fraction, which can

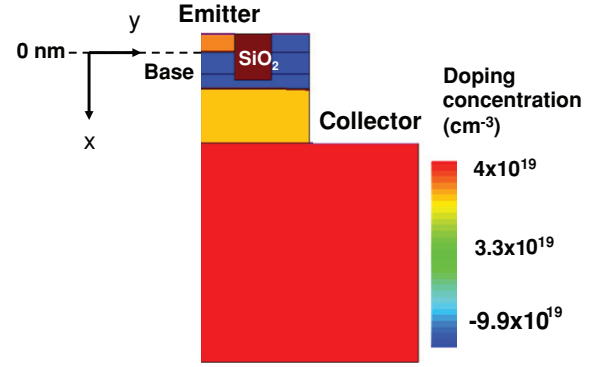


**Figure 1.** Illustration of the two-dimensional device structure of the explored SiGe HBT.

be a given parameter ranging from 0 to 0.23 [2]. Assuming the manufacturing limitation, the maximum value of Ge fraction should be less or equal to the solubility of Ge atoms in silicon, such as 0.25 [2]. In the present work, a peak base doping  $N_{\max}$  of  $1 \times 10^{19} \text{ cm}^{-3}$  at emitter edge of base and a minimum base doping  $N_{\min}$  of  $5 \times 10^{16} \text{ cm}^{-3}$  at collector edge of base have been chosen to include the heavy doping induced band gap narrowing effect in the entire base region [2].  $W_B$  is the base width of the transistor, in which a neutral base width of 100 nm is chosen.

For a SiGe HBT, the cut-off frequency  $f_t$  of a HBT is given by [16]

$$\frac{1}{2\pi f_t} = \tau_F + \frac{C_{J,BE} + C_{J,BC}}{g_m} + R_C C_{J,BC}, \quad (2)$$

where  $\tau_F$  is the forward transit time,  $C_{J,BE}$  is the base-emitter junction or depletion layer capacitance,  $C_{J,BC}$  is the base-collector junction or depletion layer capacitance,  $g_m$  is the transconductance and  $R_C$  is the collector resistance. In this model, the base transit time,  $\tau_B$ , is the major part in determining the value of  $\tau_F$  and thus governs  $f_t$ . The base transit time model in the optimization problem is given by [16], as shown below,

$$\tau_B = \int_0^{W_B} \frac{n_{i, \text{SiGe}}^2(x)}{N_A(x)} \left( \int_x^{W_B} \frac{N_A(y)}{n_{i, \text{SiGe}}^2(y) D_{n, \text{SiGe}}(y)} dy \right) dx, \quad (3)$$

where  $n_{i, \text{SiGe}}(x)$  is the intrinsic carrier concentration in SiGe, and  $D_{n, \text{SiGe}}(y)$  is the carrier diffusion coefficient of SiGe. The  $x$ - and  $y$ -directions in equation (3) are indicated in figure 1.  $D_{n, \text{SiGe}}(y)$  can be rewritten as

$$D_{n, \text{SiGe}}(y) = (1 + k_{\text{SiGe}} \text{Ge}_{\text{AVG}}) D_n(y), \quad (4)$$

where  $k_{\text{SiGe}}$  is a constant, and  $D_n(y)$  is the carrier diffusion coefficient of Si [2]. Therefore, we can also reformulate equation (2) as a function of  $N_A(x)$  [16]:

$$\begin{aligned} \frac{1}{2\pi f_{Tt}} = & \tau_B + \left( \frac{W_E P E_q, E}{2n_{i0}^2} \right) \left( \frac{\gamma^{-1}}{1 + k_{\text{SiGe}} \text{Ge}_{\text{AVG}}} \right) G_B \\ & + \left( \frac{kT \varepsilon_{\text{SiGe}}}{n_{i0}^2 2q^3 (V_{bi} - V_{BE})} \right)^{1/2}, \\ & \times \exp \left( -\frac{q V_{BE}}{kT} \right) \times N_A(0)^{1/2} G_B \left( \frac{\gamma^{-1}}{1 + k_{\text{SiGe}} \text{Ge}_{\text{AVG}}} \right) \end{aligned}$$

$$+ \frac{C_{J,BC}kT}{q^2 A_{BE} n_{i0}^2} \exp\left(-\frac{qV_{BE}}{kT}\right) \times \left(\frac{\gamma^{-1}}{1 + k_{SiGe} Ge_{AVG}}\right) G_B + \frac{W_{BC}}{2v_{sat}} + R_C C_{J,BC}, \quad (5)$$

where  $V_{BE}$  is the applied voltage across the emitter–base junction,  $V_{bi}$  is the built-in potential voltage,  $v_{sat}$  is the saturation velocity,  $n_{i0}$  is the intrinsic carrier concentration in a undoped Si,  $\epsilon_{SiGe}$  is the permittivity of SiGe,  $W_{BC}$  is the base–collector depletion width,  $W_E$  is the width of the emitter region,  $A_{BE}$  is the area of the base–emitter junction,  $k$  is the Boltzmann constant,  $T$  is the temperature (kelvin),  $PE_q$ ,  $E$  is the equilibrium concentration of holes in the emitter,  $\gamma$  is the ratio of the effective density of states in SiGe to the effective density of states in silicon and  $k_{SiGe}$  is a constant.  $G_B$  is the base Gummel number, which is also a function of  $N_A(x)$  [2]:

$$G_B = \int_0^{W_B} \frac{N_A(x)n_{i0}^2}{D_n(x)n_i^2(x)} dx. \quad (6)$$

Without loss of generality, we may assume the doping profile to be the form [2]

$$N_A(x) = bx^m, \quad 0 \leq x \leq 0.05 W_B. \quad (7)$$

Here we assume  $m = 0$  for a liner doping within 5% of the base width near the emitter–base junction. After substituting equation (6) into equation (5), the objective function can be formulated as a function of the doping profile. To figure out an ideal shape of the optimal doping profile that maximizes the cut-off frequency, we can now consider the optimization problem:

$$\begin{aligned} & \text{Minimize } \tau_B + AN_A(x)G_B(1 + K_{SiGe} Ge_{AVG})^{-1} + B \\ & \text{s.t. } N_{\min} \leq N_A(x) \leq N_{\max}, \quad 0 \leq x \leq W_B \\ & \quad 0 \leq G(x) \leq G_{\max}, \quad 0 \leq x \leq W_B \\ & \quad N_A(x) = bx^m, \quad 0 \leq x \leq 0.05 W_B \\ & \quad Ge_{AVG} = \frac{1}{W_B} \int_0^{W_B} G(x) dx \end{aligned} \quad (8)$$

where  $A$  and  $B$  are constants calculated by equation (5). The base region in (8) is then discretized to  $M$  regions,  $x_i = iW_B/M$ ,  $i = 0, 1, \dots, M-1$ , and the continue doping profile functions  $N_A(x)$  and  $G(x)$  can be transformed to  $N_A(x_i)$  and  $G(x_i)$ ,  $i = 0, 1, \dots, M-1$ , respectively and formulated as follows:

$$\begin{aligned} & \text{Minimize } \tau_B + AN_A(x_i)G_B(1 + K_{SiGe} Ge_{AVG})^{-1} + B \\ & \text{s.t. } N_{\min} \leq N_A(x_i) \leq N_{\max}, \quad 0 \leq i \leq M-1 \\ & \quad 0 \leq G(x_i) \leq G_{\max}, \quad 0 \leq i \leq M-1 \\ & \quad N_A(x_i) = bx_i^m, \quad 0 \leq i \leq 0.05M \\ & \quad Ge_{AVG} = \frac{1}{M} \sum_{i=0}^{M-1} G(x_i). \end{aligned} \quad (9)$$

Note that  $N_A(x_i)$  is the discretized variables of the doping profile in the base region;  $i$ , ranging between zero and  $M-1$ , is the uniformly spaced mesh points in the base region. Through these two sets of variables,  $N_A(x_i)$  and  $G(x_i)$ , we can co-optimize the doping profile of Si and Ge in the base region for different given  $Ge_{AVG}$  ranged from 0 to 0.23. For the original GP model in equation (9), there is no constraint

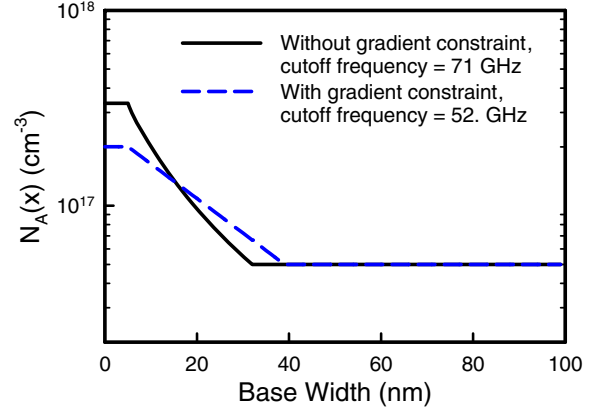


**Figure 2.** Optimized doping profile with and without a gradient constraint of the doping profile, where the Ge-dose concentration is set to be zero.

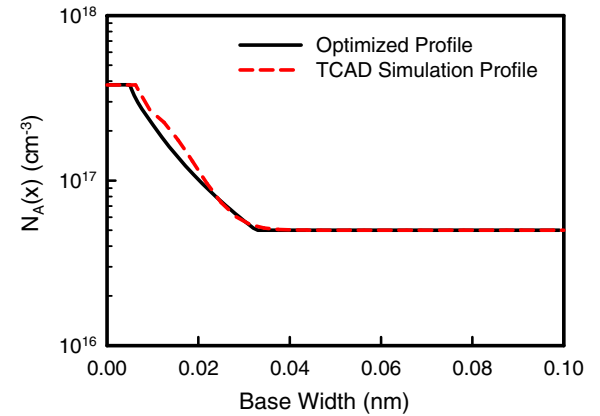


**Figure 3.** The doping profile obtained from the GP model and the 2D device simulation. The doping profile of TCAD simulation is obtained by three different ion implantation processes.

to restrict the doping profile. However, the stepwise doping profile is difficult to achieve in the realistic manufacturing process. A constraint of the doping profile is then considered [2]:

$$|N'_A(x)| \leq \alpha N_A(x), \quad (10)$$

where  $\alpha$  specifies the maximum allowed gradient and is adjustable to approximate the realistic doping profile. Figure 2 shows the doping profile of our device (0%  $Ge_{AVG}$ ) with and without a gradient constraint. The cut-off frequency of a device with a doping profile constraint is significantly smaller than that without a constraint. The incorporation of a gradient constraint of doping profile is crucial for realistic device doping profile optimization. To ensure the accuracy of the optimized doping profile, as shown in figure 3, the doping profile is implemented in our own device simulator [15, 32–36]. In device simulation, we solved a set of the two-dimensional Poisson equation as well as electron–hole current continuity equations with calibrated mobility models and generation–recombination models self-consistently. The mobility models consist of surface roughness scattering, acoustic phonon scattering and bulk mobilities. The generation–recombination models are the Shockley–Read–Hall recombination with

doping dependence and Auger recombination. After we obtained the dc operation point of a device, the ac simulation is then applied to obtain the AC characteristics of HBT. In figure 3, the solid line shows the optimized doping profile and the dashed line shows the doping profile realized in the two-dimensional device simulation. The cut-off frequency is then extracted by the 2D device simulation. The cut-off frequency in the two-dimensional device simulation approaches 70 GHz, which is very similar to the cut-off frequency in the GP model, 71 GHz. The result confirms the accuracy of the established GP model.

### 3. Results and discussion

In this section, the dependence of cut-off frequency and gain on Ge-dose and base doping profile are first discussed. Due to the strong influence of the shape and content of Ge on the base transit time, the cut-off frequency and gain of SiGe HBT are co-optimized which are subject to the aforementioned constraints.

#### 3.1. Cut-off frequency optimization

Figure 4(a) shows the SiGe HBT with various Ge-dose concentrations, 2%, 8% and 12.5%, respectively. The device with a higher Ge-dose concentration can exhibit a higher cut-off frequency. The obtained optimized doping profiles are changed with respect to different Ge-dose concentrations. The result shows a more promising characteristic of SiGe HBT than that of a pure silicon device. The Ge profiles for HBTs with various Ge-dose concentrations, 2%, 8% and 12.5%, are plotted in figure 4(b). Figure 4(c) presents the dependence of cut-off frequency as a function of Ge-dose concentration. The addition of Ge dose in silicon can provide a high cut-off frequency; however, the cut-off frequency is decreased as the Ge dose is increased and higher than 12.5%. Besides, for the Ge dose and base doping profile optimization, the background doping is also an important factor in device characteristic optimization. Figure 5(a) shows the impact of the background doping profile on the cut-off frequency. As the background doping,  $N_{\min}$ , is decreased from  $5 \times 10^{16} \text{ cm}^{-3}$  to  $3 \times 10^{16} \text{ cm}^{-3}$ , the obtained optimal cut-off frequency could be increased from 71 GHz to 85 GHz. Figure 5(b) plots the Ge profile for devices with different background doping concentrations. The Ge doping profiles are the same due to the same  $\text{Ge}_{\text{AVG}}$ . Figure 6 shows the cut-off frequency as a function of the background doping profile and Ge-dose concentration. Since the cut-off frequency is increased as the Ge-dose concentration is decreased, the device with a maximum cut-off frequency is with 12.5% Ge-dose concentration.

#### 3.2. Current gain and cut-off frequency co-optimization

In addition, the optimization of cut-off frequency and the current gain,  $\beta$ , of HBTs is crucial for communication application, which can be significantly influenced by the base doping profile. How to compromise the cut-off frequency

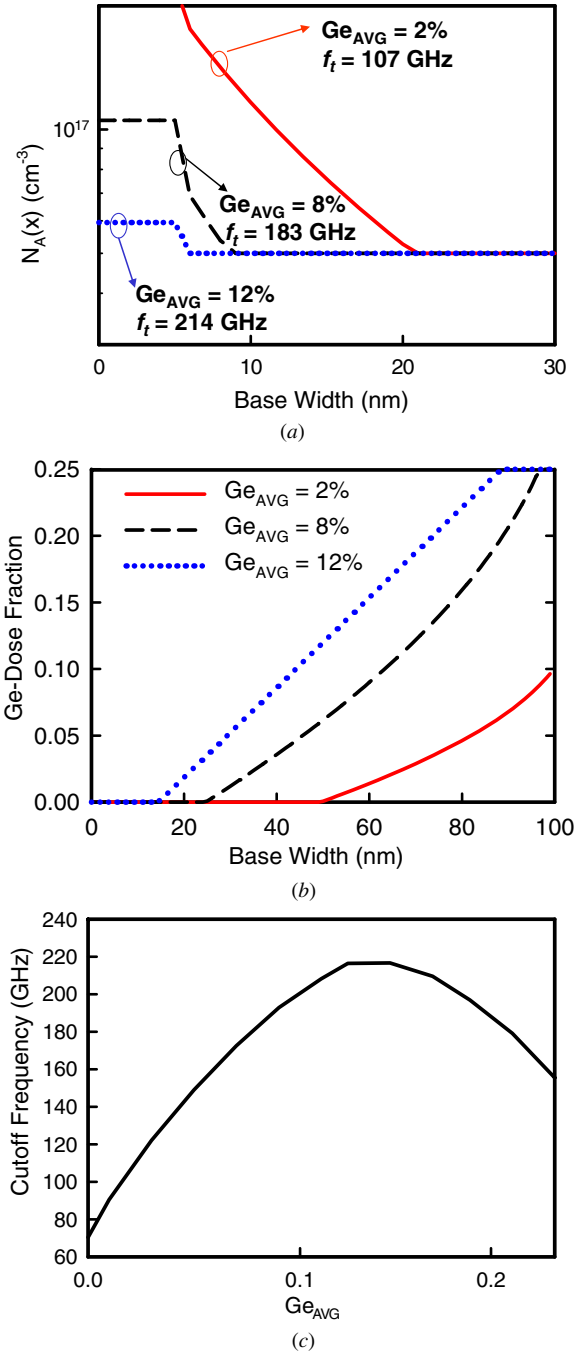


**Figure 4.** (a) Doping profile and the corresponding cut-off frequency with 2%, 8% and 12.5% Ge-dose concentrations. (b) The Ge profiles for HBTs with 2%, 8% and 12.5% Ge-dose concentrations. (c) Cut-off frequency with various Ge-dose concentrations.

and current gain of HBTs becomes a critical issue in SiGe technology. The current gain is defined by the ratio of collector and can be expressed as the ratio of Gummel numbers:

$$\beta = \frac{G_{E, \text{SiGe}}}{G_{B, \text{SiGe}}}, \quad (11)$$

where  $G_{E, \text{SiGe}}$  is the emitter Gummel number and  $G_{B, \text{SiGe}}$  is the base Gummel number. Since the emitter Gummel number depends mostly on the emitter doping profile, it



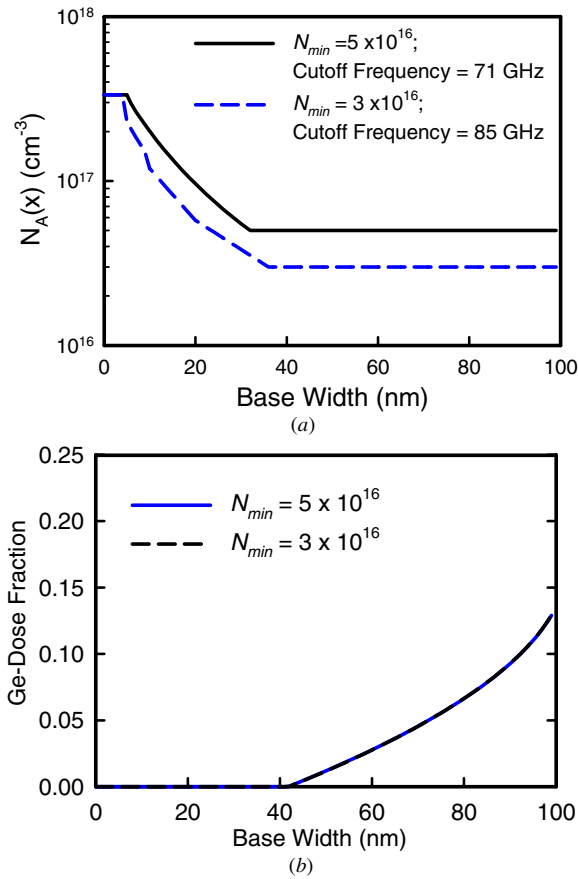


**Figure 5.** (a) Doping profile of decreasing background doping to  $3 \times 10^{16} \text{ cm}^{-3}$  for 3% Ge content. (b) Doping profile of Ge for different background doping concentrations of Si.

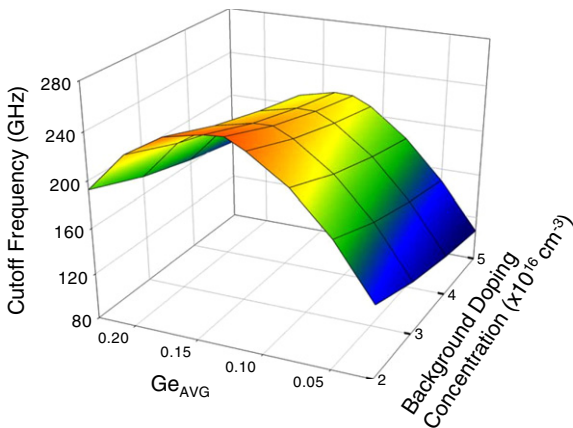


**Figure 6.** The cut-off frequency as a function of Ge-dose and background doping concentrations.

can be treated as a positive constant in the optimization flow. For the base Gummel number, the dependence of the Gummel number on the base doping profile has been studied in equation (6). Therefore, the relationship and equation (11) are then transformed as the current gain constraint and plugged into the GP model. Figure 7 shows the cut-off frequency as a function of the current gain. Since the cut-off frequency is related to the current gain and bandwidth, the obtained cut-off

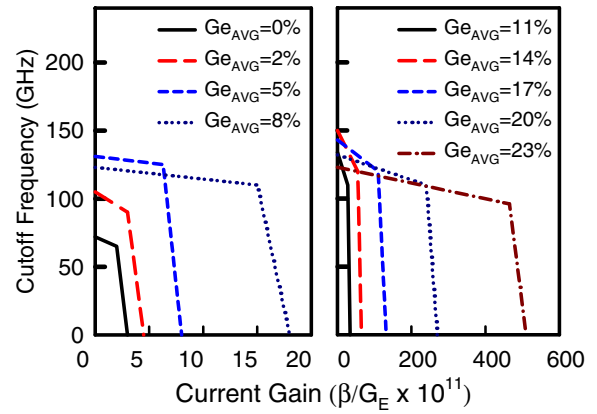


**Figure 7.** The maximized current gain constraint can add for 0%, 5% and 8% Ge content.

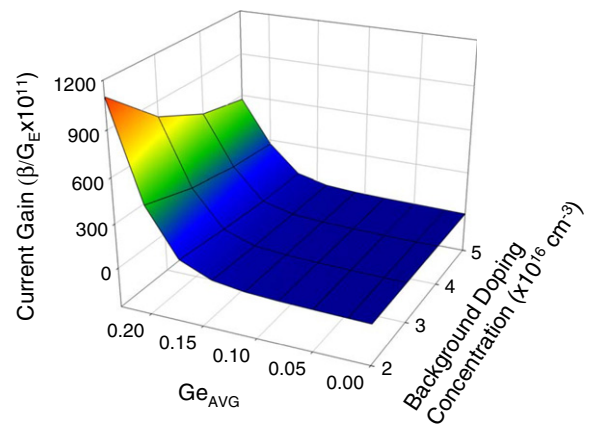


**Figure 8.** The maximum current gain constraint, which is added for every Ge content and background doping to maintain sufficient cut-off frequency.

frequency will be smaller with a higher current gain constraint. The relation between cut-off frequency and current gain varies with different Ge-dose concentrations. The device with 14% Ge-dose concentration exhibits the highest cut-off frequency. However, to obtain the maximum current gain, the device with the highest Ge-dose concentration exhibits a favorable characteristic. Moreover, the results show that the device with a higher Ge-dose concentration could provide a higher gain and thus releases the design constraint. For each of the Ge content, the cut-off frequency is decreased with increasing current gain constraint and then dropped significantly. The tuning point, in which the current gain constraint starts to significantly reduce the cut-off frequency, is decisive in obtaining the maximum current gain with sufficient cut-off frequency. Therefore, by careful selection of the maximum current gain constraint, we could find the optimal current gain constraint,  $\beta/G_{E, \text{SiGe}} \times 10^{11}$ , with sufficient cut-off frequency, as shown in figure 8, where the lower background doping concentration and higher Ge-dose concentration may provide the largest current gain.

As shown in figure 6, it is found that 12.5% Ge-dose concentration and  $2 \times 10^{16} \text{ cm}^{-3}$  background doping concentration can maximize the cut-off frequency. The

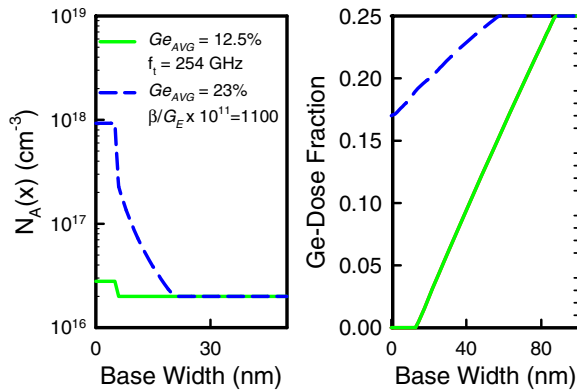


**Figure 9.** Optimal Si and Ge doping profile for  $f_i$  maximize and maximize current gain constraint.

highest cut-off frequency can reach 254 GHz. On the other hand, for obtaining the maximum current gain, as shown in figure 8, the Ge-dose concentration is about 23% and the background doping is about  $2 \times 10^{16} \text{ cm}^{-3}$ , where the maximized current gain constraint  $\beta/G_{E,\text{SiGe}} \times 10^{11} = 1100$ , and the value of current gain  $\beta$  is about 1200. The obtained optimal doping profile and Ge-dose concentration are plotted in figure 9. Result shows that for the SiGe HBTs, the triangular Ge profiles are best suited to achieve the minimum base transit time and trapezoidal Ge profiles are best suited to get high current gain in SiGe HBTs, which matches the practical design consideration of SiGe HBTs [18]. The design of Ge-dose concentration for obtaining high cut-off frequency and high current gain is rather different. Therefore, to find a compromise between high cut-off frequency and high current gain, the product of cut-off frequency and current gain is considered as a new object function. The optimized result is shown in figure 10, similar to the result of current gain, shown in figure 8; the device with a higher Ge-dose concentration and a lower background doping concentration exhibits the best result. The optimal condition for maximum cut-off frequency–current gain product is at the point of  $\text{Ge}_{\text{AVG}} = 23\%$  and  $N_{\text{min}} = 2 \times 10^{16} \text{ cm}^{-3}$ . The correspondent optimal doping profile and Ge profile are the dashed lines in figure 9. We note that the object function, which is composed by the cut-off frequency and the current gain, could be adjusted according to designer's interest.

#### 4. Conclusions

In this study, the cut-off frequency and the current gain of SiGe HBT have been optimized via a geometric programming approach. The design of the doping profile and the Ge concentration in the base region has been transformed into a convex optimization problem, and solved in a cost-effective manner. The major contributions of this study, compared with [2], consist of

- (1) transformation of the formula of cut-off frequency into a GP form, and optimal doping profiles of Si and Ge were simultaneously achieved;
- (2) the cut-off frequency optimization with the gradient constraint of doping profile was implemented;

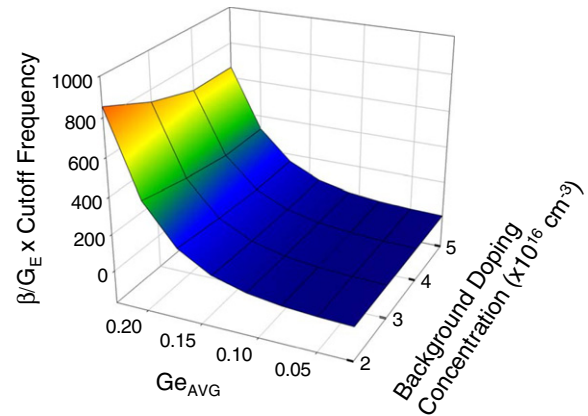


**Figure 10.** Co-optimization of cut-off frequency and current gain for the SiGe HBTs.

- (3) adjustable background doping of Si for the corresponding optimization problem was advanced;
- (4) considering the current gain constraint, the corresponding high current gain and cut-off frequency were thus achieved; and
- (5) confirmation of all results with TCAD device simulation.

Our preliminary result has shown that a 23% Ge fraction may maximize the current gain; besides, a 12.5% Ge fraction can maximize the cut-off frequency, where 254 GHz cut-off frequency has been achieved. For the SiGe HBTs, the triangular Ge profiles are best suited to achieve the minimum base transit time and trapezoidal Ge profiles are best suited to get high current gain in SiGe HBTs. The accuracy of the adopted optimization technique was first confirmed by comparing with two-dimensional device simulation; consequently, the employed approach is computationally efficient and guarantees to always find the globally optimal solution. For concurrent optimization of multiple dopants in a device channel, unlike other optimization approaches, which cycle through optimizing each dopant species with the others fixed, this approach may give the optimal solution without the iteration. The GP formulation of device characteristics provides an alternative way to design SiGe HBTs. We are currently applying the GP approach for multi-finger HBT optimization.

#### Acknowledgment

This work was supported in part by Taiwan National Science Council (NSC) under Contract NSC-97-2221-E-009-154-MY2.

#### References

- [1] Khanduri G 2007 Simultaneous optimization of doping profile and Ge-dose in base in SiGe HBTs *IEEE Southeast Conf.* pp 579–83
- [2] Joshi S, Boyd S and Dutton R 2005 Optimal doping profiles via geometric programming *IEEE Trans. Electron Devices* **52** 2660–75

- [3] Marshak A-H 1967 Optimum doping distribution for minimum base transit time *IEEE Trans. Electron Devices* **14** 190–4
- [4] Szeto S and Reif R 1989 Reduction of  $f$  by nonuniform base bandgap narrowing *IEEE Electron Device Lett.* **10** 341–3
- [5] Winterton S-S, Searles S, Peters C-J, Tarr N-G and Pulfrey D-L 1996 Distribution of base dopant for transit time minimization in a bipolar transistor *IEEE Trans. Electron Devices* **43** 170–2
- [6] Kumar M-J and Patri V-S 2001 On the iterative schemes to obtain optimum base profiles for transit time minimization in a bipolar transistor *IEEE Trans. Electron Devices* **48** 1222–4
- [7] Wijnen P-V and Gardner R-D 1990 A new approach to optimizing the base profile for high-speed bipolar transistors *IEEE Electron Device Lett.* **11** 149–5
- [8] Rinaldi P and Schättler H 2002 Minimization of the base transit time in semiconductor devices using optimal control *Int. Conf. Dynamical Systems Differential Equations* pp 1–10
- [9] Kroemer H 1985 Two integral relations pertaining to the electron transport through a bipolar transistor with a nonuniform energy gap in the base region *Solid-State Electron.* **28** 1101–3
- [10] Hareme D-L, Comfort J-H, Cressler J-D, Crabbe E-F, Sun J-Y-C, Meyerson B and Tice T 1995 Si/SiGe epitaxial-base transistors: Part I. Materials, physics, and circuits *IEEE Trans. Electron Devices* **42** 455–68
- [11] Patri V-S and Kumar M-J 1998 Profile design considerations for minimizing base transit time in SiGe HBTs *IEEE Trans. Electron Devices* **45** 1725–31
- [12] Suzuki K 1991 Optimum base doping profile for minimum base transit time *IEEE Trans. Electron Devices* **38** 2128–33
- [13] Lu T-C and Kuo J-B 1993 A closed-form analytic forward transit time model considering specific models for bandgap-narrowing effects and concentration-dependent diffusion coefficients for BJT devices operating at 77 K *IEEE Trans. Electron Devices* **40** 766–72
- [14] Khanduri G and Panwar B 2006 Study of base doping profile effects on SiGe heterojunction bipolar transistors performance for all levels of injection *Semicond. Sci. Technol.* **21** 486–93
- [15] Li Y and Huang K-Y 2003 A novel numerical approach to heterojunction bipolar transistor circuit simulation *Comput. Phys. Commun.* **152** 307–16
- [16] Taur Y and Ning T 1998 *Fundamentals of Modern VLSI Devices* (Cambridge, UK: Cambridge University Press)
- [17] Ashburn P 2003 *SiGe Heterojunction Bipolar Transistors* (New York: Wiley)
- [18] Kim K, Heo J, Kim S, Mangalaraj D and Junsin Y 2002 Optimum Ge profile for the high cut-off frequency and the DC current gain of an SiGe HBT for MMIC *IEEE Trans. Electron Devices* **40** 584–7
- [19] Kortanek K, Xu X and Ye Y 1976 An infeasible interior-point algorithm for solving primal and dual geometric programs *Math. Program.* **76** 155–81
- [20] Avriel M, Dembo R and Passy U 1975 Solution of generalized geometric programs *Int. J. Numer. Methods Eng.* **9** 149–68
- [21] Bightler C-S and Phillips D-T 1976 *Applied Geometric Programming*. (New York: Wiley)
- [22] Duffin R-J 1970 Linearizing geometric programs *SIAM Rev.* **12** 211–27
- [23] Duffin R-J, Peterson E-L and Zener C 1967 *Geometric Programming—Theory and Applications* (New York: Wiley)
- [24] Ecker J 1980 Geometric programming: methods, computations and applications *SIAM Rev.* **22** 338–62
- [25] Anstreicher K and Vial J-P-H 1994 On the convergence of an infeasible primal-dual interior-point method for convex programming *Optim. Methods Softw.* **4** 273–83
- [26] Balm O, Goffin J-L, Vial J-P-H and Merle O-D-U 1994 Experimental behavior of an interior point cutting plane algorithm for convex programming: an application to geometric programming *Discrete Appl. Math.* **49** 2–23
- [27] Charnes A, Cooper W-W, Golany B and Masters J 1998 Optimal design modification by geometric programming and constrained stochastic network models *Int. J. Syst. Sci.* **19** 825–44
- [28] Kyparsis J 1998 Sensitivity analysis in posynomial geometric programming *J. Optim. Theory Appl.* **57** 57–85
- [29] Chiang M, Chan B and Boyd S 2002 Convex optimization of output link scheduling and active queue management in QoS constrained packet switches *Proceedings of the IEEE International Conf. on Comm.* pp 2126–30
- [30] Scoot C-H and Jefferson T-R 1995 Allocation of resource in project management *Int. J. Syst. Sci.* **26** 413–20
- [31] GGPLAB A simple Matlab toolbox for geometric programming [Online] <http://www.stanford.edu/~boyd/ggplab/>
- [32] Li Y, Sze S M and Chao T-S 2002 A practical implementation of parallel dynamic load balancing for adaptive computing in VLSI device simulation *Eng. Comput.* **18** 124–37
- [33] Li Y and Yu S-M 2004 A two-dimensional quantum transport simulation of nanoscale double-gate MOSFETs using parallel adaptive technique *IEICE Trans. Inf. Syst.* **87** 1751–8
- [34] Li Y, Huang J-Y and Lee B-S 2008 Effect of single grain boundary position on surrounding-gate polysilicon thin film transistors *Semi. Sci. Tech.* **23** 015019
- [35] Li Y, Hwang C-H, Chen C-C, Yan S and Lou J-C 2008 UV illumination technique for leakage current reduction in a-Si:H thin film transistors *IEEE Trans. Electron Devices* **55** 3314–8
- [36] Li Y and Hwang C-H 2009 DC Baseband and high-frequency characteristics of silicon nanowire field effect transistor circuit *Semi. Sci. Tech.* **24** 045004